Soft Magnetic Materials: Synthesis, Characterization, and Applications Introduction

**Review Summary: Soft magnetic materials for a sustainable and electrified world**

**Background:** Soft magnetic materials and their related devices (inductors, transformers, and electrical machines) are often overlooked, however, they play a key role in the conversion of energy throughout our world. Conversion of electrical power includes the bidirectional flow of energy between sources, storage, and the electrical grid and is accomplished using power electronics. Electrical machines (motors and generators) transform mechanical energy into electrical energy and vice versa. The introduction of wide band gap (WBG) semiconductors is allowing power conversion electronics and motor controllers to operate at much higher frequencies. This reduces the size requirements for passive components (inductors and capacitors) in power electronics and enables more efficient, high rotational speed electrical machines. However, none of the soft magnetic materials available today are able to unlock the full potential of WBG based devices.

Since the 1800s, when iron was the only soft magnetic material available, metallurgists, materials scientists, and others have been periodically introducing improved materials. The invention of silicon (electrical) steel in 1900 was a notable event for soft magnetic materials. Still today, silicon steel dominates the global market of soft magnets, and is the material of choice for large scale transformers and electrical machines. However, its low electrical resistance makes it subject to large losses from eddy currents, particularly as operating frequencies are increased. This leaves the soft magnetic community looking to other materials to meet the needs of newer high frequency devices.

**Advances:** There are several soft magnetic materials that show promise for high frequency operation. As oxides, soft ferrites stand out from other magnetic materials since they are insulating. They are therefore excellent at reducing losses from eddy currents. However, they suffer from a saturation magnetization ($M_s$) that is almost a factor of four less than silicon steel. This substantially limits the power density in devices designed using soft ferrites and therefore limits their application. The current state of the art materials are the amorphous and nanocrystalline alloys, which were invented in 1967 and 1988, respectively. Their unique nanostructure and extremely thin laminations work together to keep eddy current losses low even at high frequencies. However, fabricating parts by cutting and then stacking or winding extremely thin and brittle laminations can be challenging. Composites are the newest class of soft magnetic materials, and in the field of soft magnetics, they are referred to as powder cores or soft magnetic composites (SMCs). They are comprised of micrometer sized particles coated consolidated at high pressures with an insulating binder. Although their performance is rather modest their isotropic nature makes them well suited for use in rotating electrical machines.

**Outlook:** The need for improved soft magnets capable of efficient operation at high frequencies is capturing the attention of a growing number of researchers. Improvements to existing materials are being developed by some researchers, while others are looking at dramatically new

approaches. Even though ferrites were invented in the 1940s, grain boundary engineering and new syntheses amenable to integrated manufacturing are being pursued. The nanocrystalline and amorphous materials are constantly being improved through increases in $M_s$ and the introduction of alloys that are more amenable to the fabrication of large scale parts. Powder cores have opened the door for nanoparticle based composites, which can be fabricated not just with top-down but also bottom-up approaches. A well designed nanocomposite has the potential for negligible losses over specific temperature and frequency ranges. In all materials advanced characterization techniques will be paramount to understanding the relationship between nanostructure and magnetization reversal, which will then enable the design of improved soft magnets.

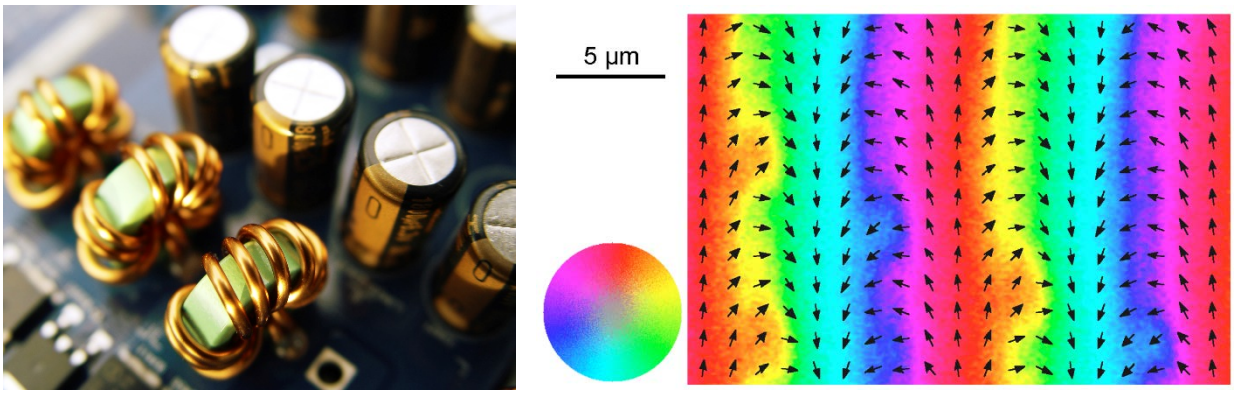


**Fig. 0. Two views of soft magnetic materials. (Left)** A row of three wound toroidal inductors mounted on a printed circuit board. **(Right)** Magneto-optical Kerr effect (MOKE) image of the magnetization pattern on the surface of an amorphous alloy soft magnet [From (*1*)].

# Soft magnetic materials for a sustainable and electrified world

Josefina M. Silveyra[1], Enzo Ferrara[2], Dale L. Huber[3], Todd C. Monson[4*]

1. Laboratorio de Sólidos Amorfos, INTECIN, Facultad de Ingeniería, Universidad de Buenos Aires - CONICET, Buenos Aires, Argentina
2. Istituto Nazionale di Ricerca Metrologica (INRIM), Torino, Italy
3. Center for Integrated Nanotechnologies, Sandia National Laboratories, Albuquerque, NM 87185, USA
4. Sandia National Laboratories, Albuquerque, New Mexico 87185, USA

* Corresponding author. E-mail: tmonson@sandia.gov

**Soft magnetic materials are key to the efficient operation of the next generation power electronics and electrical machines (motors and generators). Many new materials have been introduced since Michael Faraday's discovery of magnetic induction, when iron was the only option. However, as wide band gap (WBG) semiconductor devices become more common in both power electronics and motor controllers, there is an urgent need to further improve soft magnetic materials. These improvements will be necessary to realize the full potential in efficiency, size, weight, and power (SWaP) of high frequency power electronics and high rotational speed electrical machines. Here, we will provide an introduction to the field of soft magnetic materials and their implementation in power electronics and electrical machines. Additionally, we will review the most promising choices available today and describe emerging approaches to create even better soft magnetic materials.**

As we transition to both a more electrified world and renewable sources of energy, efficient power conversion will take on an increasingly important role to manage the bidirectional flow of power between sources (solar arrays, wind turbines, or other power plants), storage, and the electrical grid. Power conversion can also describe the transformation between mechanical energy into electrical energy, which is being accomplished to a greater extent with electrical machines (both motors and generators). Electrical machines are a vital part of industry worldwide and are becoming very important to all forms of transportation. In both cases of power conversion described above, the advancing field of wide band gap (WBG) semiconductors is an enabling technology. Their high switching speed and increased operating temperature are driving faster and more compact power conversion electronics and motor controls. Additionally, WGB devices have decreased cooling requirements compared with silicon electronics.

In the field of power electronics, however, efforts to modernize the passive components (transformers, inductors, and capacitors) have lagged compared with the abundance of work focusing on semiconductor switches. Here, we focus on the magnetic-based passive devices and address the challenges facing transformers and inductors, which both require a soft (low coercivity) magnetic core to achieve high-power densities. Advances in the magnetic materials

used in transformers and inductors will be equally beneficial to electrical machines. Thus, we will also discuss how electrical machines could realize substantial improvements in power density and efficiency through improved soft magnetic materials. Given all of the applications of power electronics and electrical machines, we will see that soft magnets are ubiquitous. For that reason, research focusing on improving soft magnetic materials could have a huge impact on global energy efficiency.

## Fundamentals of soft magnets

Before continuing our discussion of soft magnets, it is important to describe the basic characteristics of a magnetization curve and define some key magnetic parameters. The defining relation between the three magnetic field vectors is:

$$\mathbf{B} = \mu_0(\mathbf{H} + \mathbf{M}) = \mu_0\mathbf{H} + \mathbf{J} \quad (1)$$

Where $\mu_0$ is the magnetic permeability of vacuum, **B** is the magnetic flux density or induction, **H** is the magnetic field, **M** is the magnetization or volume density of the magnetic moment, and **J** ($\mu_0$**M)** is the magnetic polarization. In materials science, it is more common to represent magnetic response in terms of **M**, whereas device technology most often uses **J**, which is analogous to the polarization (**P**) in dielectric materials. The response of magnetic materials can be represented in terms of **M**(**H**), **B**(**H**), or **J**(**H**). Within this magnetic response are embedded a complex mix of processes that include domain wall motion, rotation of magnetic moments, and eddy current losses (*2*).

Several key parameters for a soft magnetic material can be extracted from its magnetization curve. The magnetic susceptibility is defined as $\chi$=M/H and the relative magnetic permeability is defined as $\mu_r=\mu/\mu_0=B/\mu_0H=(1+\chi)$. The susceptibility (and also $\mu_r$) can be measured at any point along the magnetization curve. However, most often, the value of $\chi$ or $\mu_r$ is measured starting at the point of zero field and reported as the initial susceptibility or permeability ($\chi_i$ or $\mu_i$, respectively). Both $\mu_r$ and $\chi$ are indications of how much magnetic field is required to change the direction of the magnetization in a sample. Other key parameters include a sample's saturation magnetization ($M_s$) which is the sample's maximum magnetization, magnetic remanance ($M_r$) or magnetization that remains after all external field is removed, and coercive field ($H_c$) or the strength of the opposing field required to remove a sample's magnetization after saturation. Figure. 1 displays a magnetization curve, M(H), for a soft magnetic material with $M_s$, $M_r$, $H_c$, and $\chi_i$ labeled.

Three other properties of magnetic materials are also important descriptors. A magnetic material's anisotropy (K), which is the energy difference between the preferred and non-preferred directions of magnetization within a material. Magnetocrystalline anisotropy is an intrinsic property of a material determined by its crystalline structure and spin–orbit coupling. Although magnetocrystalline anisotropy can be described with series expansions with terms out to many orders, most often the first-order constant ($K_1$) is sufficient for calculations. The second

property is magnetostriction ($\lambda$), which is a material's dimensional change as a function of applied magnetic field. Magnetostriction can be a source of loss through the unwanted conversion of electromagnetic energy into mechanical energy. This effect results in the humming sound created by the magnetic cores of transformers. Additionally, there can be a coupling between a material's magnetization and strain (magnetoelastic coupling). This coupling can result in an additional anisotropy term, stress anisotropy ($K_\sigma$). A material's overall or effective anisotropy ($K_{eff}$) approximately follows a proportional relation with $H_c$ while the initial susceptibility $\chi_i$ is inversely proportional to K (*3*). Finally, the Curie temperature ($T_c$) is the temperature above which a material loses its magnetic order and becomes paramagnetic. $T_c$ is an important parameter for power electronics and electrical machines, which often operate at high temperatures and where space for active cooling may not be available.

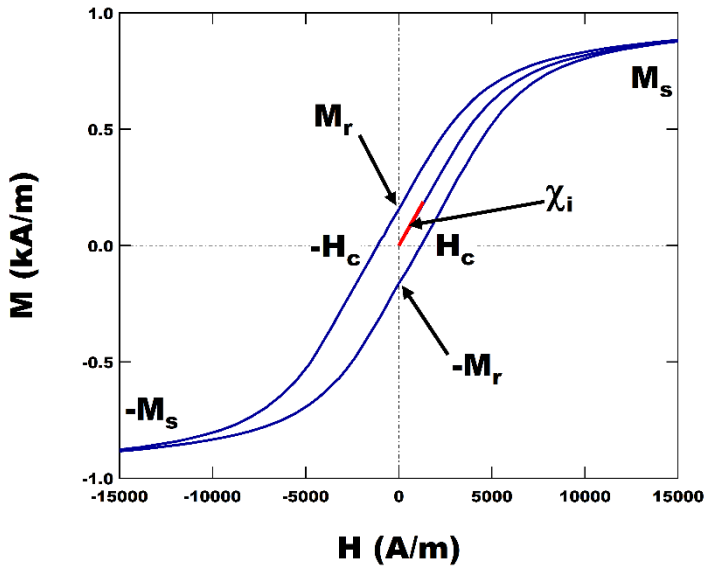


**Fig. 1. Magnetization curve for a soft magnet.** A magnetization curve, M(H), for a soft magnetic material with $M_s$, $M_r$, $H_c$, and $\chi_i$ labeled. The sample is Metglas 2605SA1 amorphous alloy and was provided courtesy of Metglas.

Most often, when people consider magnets, they think about permanent (hard) magnets. Permanent magnets have a large $H_c$ (> 1000 A/m) and high $M_r$ that allows them to retain a large magnetization after being magnetized. This property allows hard magnets to attract and repel other magnets and to even magnetize other materials (such as the steel in your refrigerator door). However, for the inductive applications found in power electronics and electrical machines, permanent magnets are not useful. Instead, these applications require soft magnets that have a low $H_c$ (< 1000 A/m) and very little $M_r$. Inductive applications are based on the ability to rapidly switch the magnetization of a material with a magnetic field created by current carrying coils of wire. The high $\mu_r$ of a soft magnet concentrates (by orders of magnitude greater than an air core) the magnetic field lines inside the windings of an inductor or electrical machine, and boosts the performance of the inductive device by allowing it to store more energy in the form of magnetic flux density. An increase in energy density is precisely what is needed for emerging power

electronics and electrical machines where size, weight, and power (SWaP) are often the most important metrics. For this reason, increasing the $M_s$ of soft magnets can have a positive impact on SWaP by increasing the maximum field at which a magnetic device can operate.

## Energy losses

The increase in energy density that soft magnetic core materials bring to inductive devices do not come without a cost, as core materials can also be a place of energy loss, particularly as operating frequencies increase. Hysteretic losses occur through a magnetic material's coercivity. Every time a magnet completes a full cycle of its magnetization curve, the area inside the curve is a measure of the energy lost. Thus, as operating frequencies increase, even magnets with low coercivity can become quite lossy. The second major loss mechanism for soft magnetic devices are eddy currents, which are closed paths of electrical current generated in a conductor created by a time-varying magnetic field. These current loops create a magnetic field in opposition to the change in magnetic flux (according to Faraday's law of induction.) Power losses from eddy currents roughly scale as the operating frequency squared, so they can become the dominant source of energy loss at high switching rates. Mitigating both hysteretic and eddy current losses consumes a large portion of the resources dedicated toward improving soft magnetic materials.

Theoretical treatment of magnetic losses can be quite complicated as magnetic materials are not continuous and instead contain magnetic domains, domain walls, and a complex distribution of eddy currents. One of the first models on magnetic losses was developed by Williams, Shockley, and Kittel (WSK model) (*4*). Their model, which only applied to 180° Bloch walls in monocrystalline silicon steel, was broadened to describe loss behavior in a grain oriented (GO) silicon steel sheet by Pry and Bean (*5*). Bertotti took a statistical approach and applied the concept of loss separation in developing the Statistical Theory of Losses (STL) (*6*). According to the STL, energy loss, W(f), at a given magnetizing frequency f and peak magnetic polarization $J_p$, is the sum of three components: hysteresis loss ($W_h$), classical loss ($W_{cl}$), and excess losses ($W_{exc}$). These terms correspond, respectively, to the residual energy dissipated in the limit $f \to 0$, the loss component calculated by Maxwell's equations assuming the material is magnetically homogeneous (absent of domains), and the energy loss associated with the large-scale motion of the domain walls (*6*).

$$W(f) = W_h + W_{cl}(f) + W_{exc}(f) \tag{2}$$

Although all three components, at their root cause, are the result of eddy current mechanisms (only at different space–time scales) (*2*) the classical loss is the term most closely associated with eddy current losses and can be written as:

$$W_{cl} = (\pi^2/6)\cdot\sigma d^2 J_p f \tag{3}$$

where $\sigma$ is the conductivity of the material, d is the lamination thickness (this assumes that d is greater than the skin depth, which may not be the case at high frequencies), $J_p$ the peak

polarization, and f the frequency. The squared dependence on d is why many soft magnetic materials, in particular, steels, amorphous alloys, and nanocrystalline alloys, are fabricated into parts as wound tape or stacked laminations. Excess loss, which is associated with large-scale domain wall motion, is described in more detail elsewhere, but increases as a function of $f^{3/2}$ (*7-9*). Because a substantial portion of losses arise from domain wall motion, developing finer control over the micro and nanostructure of magnetic materials can reduce impediments to domain wall motion and overall losses. Figure 2 demonstrates an example of an impediment to domain wall motion, capturing two different pinning sites using magneto-optical Kerr effect (MOKE) imaging.

The STL complies, in general, with experiments up to frequencies where magnetic shielding strongly enters into play. Beyond this limit (> 1 MHz) more complex formulations, exploiting hysteresis modeling (such as the Dynamic Preisach Model), and numerical calculations are usually used (*10-13*). Measurements can consistently proceed up to radio frequencies, starting from quasi-static characterization, and the theoretical approach can be fully applied under a quasi-linear constitutive magnetic equation, which implies low or very low $J_p$ (within the Rayleigh region).

## Power electronics

A key benefit of the higher operating frequencies enabled by wide band gap semiconductors is a decrease in the inductive and capacitive requirements for a given circuit. As an example, the undesired alternating voltage component, or ripple voltage ($V_{ripple}$) in a step-down (buck) DC-to-DC converter is given by:

$$\frac{V_{ripple}}{V_{out}} = \frac{1-D}{8LCf^2} \tag{4}$$

where $V_{out}$ is the converter output voltage, D is the duty cycle, L is the circuit inductance, C the capacitance, and f is the operating frequency. The size of the inductor and capacitor can be reduced substantially while keeping the ripple voltage constant by increasing the operating frequency. Similar reductions in the footprint of passive devices can be realized in almost all power electronics circuitry.

Advances in power electronics are also enabling the development of intelligent and agile "solid–state transformers" or SSTs, which operate at a much higher frequency (> 1 kHz) and shrink the size the conventional 60-Hz transformer by a factor of ten or more (*14, 15*). Although WBG semiconductors enable the reduction of soft magnetic components, none of the magnetic materials available today can fully unlock the potential of WBG devices(*16*).

## Electrical machines

Electric motor driven systems are the single largest consumer of electricity, accounting for over 40% of the electrical energy generated globally(*17*). Even small efficiency

improvements in electric machines will have a large impact on energy savings. According to the International Energy Agency, if by 2030 all industries adopted the already available high efficiency technologies for their electric motor driven systems, energy savings would exceed 300 billion kWh, helping to reduce 200 Mt of $CO_2$ emissions per year (*17*). There would also be financial benefits from more efficient motors, because energy consumption is typically responsible for over 90% of the overall cost of a motor (*17, 18*). Electric cars, aircraft, and spacecraft need higher efficiencies and power densities, not only because energy storage is limited, but since volume and weight are also crucial.

As electric machines get smaller, design engineers are facing the growing challenge of keeping the components cool. Overheating deteriorates the properties of most materials (such as insulators, coils, and permanent magnets) and reduces the service life of the device. Fewer losses would reduce cooling loads, permit the use of a smaller fan at the end of the rotor, and further decrease the size of the machine.

In the conversion between electrical energy and mechanical energy, electrical machines experience several loss mechanisms including mechanical, winding or coil (also referred to as copper), and core (also referred to as iron). Core losses, which are due to ferromagnetic hysteresis and eddy currents in the stator and rotor, are independent of load. Core losses depend on the properties of the magnetic material, the flux density, and the rate of change of the flux density (i.e. switching frequency). Core losses have typically been estimated to account for 15 to 25% of the total loss (*19*). However, this percentage increases substantially as machines are operated at higher speeds. For example, core losses account for 59% of the total loss in a 110 kW machine operating at 51,000 rpm (*20*).

Operation at much higher speeds, which is enabled by advanced motor controls driven by new WBG semiconductors, is another approach to increasing power. The mechanical power of a motor is defined as the rotational speed times the torque, or $\omega \cdot T$. By increasing rotational speed, either the power density can be increased or the size of the motor can be decreased, which leads to a reduction of the critical rare-earth elements in permanent magnet motors (*21*). Additionally, gearboxes can be eliminated in various applications that require high rotational speeds. A major problem with using high speeds is that core losses increase as a function of the switching frequency, which is where advances in soft magnetic materials can influence performance improvements in electrical machines.

## Brief history of soft magnetic materials

Ever since Michael Faraday demonstrated electromagnetic induction in 1831, there has been a continuing evolution of soft magnetic materials. Faraday's natural choice of core material was iron, which has the highest room temperature $M_s$ of any element in addition to a large $\mu_r$ and fairly low $H_c$. However, even in a simple material comprised of a single element there was room for considerable improvement. It was discovered that annealing iron not only improved its

mechanical properties but also decreased its coercivity through stress relief, making it better suited for use in inductive applications.

Seeking even better performance, scientists and engineers looked for ways to improve upon the properties of soft iron. In 1900, Robert Hadfield, a metallurgist from England, invented nonoriented silicon steel by adding up to 3% silicon to iron and increasing its electrical resistivity ($\rho$) while also increasing $\mu_r$ (*22*). American metallurgist Norman Goss invented grain-oriented silicon steel in 1933 by promoting grain growth along a crystalline direction of low anisotropy, increasing $\mu_r$ even further (*22*). Even today, silicon (or electrical) steels account for a major share of the global soft magnet market because of their high $M_s$ and relatively low cost (*2*). The most common applications for silicon steel are large-scale transformers (grain-oriented silicon steel) and electrical machines (isotropic nonoriented silicon steel is preferred for rotating machines), where its economical price is a huge benefit. However, a low $\rho$ (~ 0.5 $\mu$ohm·m) (*23*) makes silicon steels lossy at high frequency. Recently, electrical steel manufacturers have developed a path to increase the silicon content of their steel to 6.5% using a chemical vapor deposition (CVD) process (*24*). This approach increases $\rho$ to 0.82 $\mu\Omega$·m but still leaves other materials as better choices for high-frequency power electronics and high rotational speed electrical machines.

In the 1910s, Gustav Elmen at Bell Laboratories experimented with nickel–iron alloys and discovered the nickel-rich (78%) permalloy composition (*25*). A major advantage of permalloy is its high $\mu_r$ (up to 100,000). Nickel–iron alloys are still used in some specialty inductive applications today but are not common in power electronics and electrical machines because they have high eddy current losses, and the addition of nickel decreases $M_s$. With the addition of a small amount of molybdenum (2%) to permalloy, molypermalloy powder (MPP) can be produced (*26*). MPP is used to fabricate the lowest loss powder cores (*26, 27*), which will be discussed in more detail below.

In the late 1940s magnetically soft ferrites were invented by J. L. Snoek (*28*). These materials are competitive because of their very high electrical resistivities ($10 - 10^8$ $\mu$ohm·m), which make them effective at suppressing eddy current losses. Additionally, because they are produced with ceramic processing techniques and abundant materials, ferrite parts can be produced at a very low cost. The high $\rho$ and affordability of soft ferrites keeps these materials in high demand for inductive applications, including those at high frequency. In fact, their share of the global market in soft magnets is second only to silicon steel (*2*). They do suffer from a relatively low $M_s$ (nearly a quarter of that of silicon steel), which limits the energy density of inductive elements containing a ferrite core.

In 1967, a new class of materials, amorphous alloys, were invented (*29*). By the mid-1970s, interest in iron and cobalt based amorphous alloys was surging and they began finding their way into applications. Through the elimination of any long range order, coercivity is substantially reduced in these alloys. In 1988, researchers at Hitachi included Nb and Cu

additives and added an annealing step to the production of amorphous alloys to produce small and closely spaced crystallites of iron or cobalt (on the order of 10 nm in diameter) within a matrix of amorphous material (*30*). This was the inception of the nanocrystalline soft magnetic alloys. The formation of isolated transition metal crystallites reduced the eddy current losses of these materials in comparison to amorphous alloys. Both amorphous and nanocrystalline alloys are gaining market share in high-frequency power electronics and electrical machines today because of their low losses and competitive $M_s$. Despite a higher initial cost than silicon steel, these advanced alloys can reduce the total lifetime costs of power electronics and electrical machines, thanks to reduced losses.

In the early 1990s, powder cores (also known as soft magnetic composites or SMCs) gained acceptance in some soft magnetic applications (*2, 31*). These materials combine magnetic particles, anywhere between approximately 1 to 500 μm in diameter, and either coat or mix them with an insulating material before consolidating with high pressures (MPa to even GPa pressures). Heat can also be applied either during or after densification to improve magnetic properties. The magnetic particles are most often Fe powders but can also consist of alloys such as MPP (mentioned earlier), Fe–P, Fe–Si, or Fe–Co. Because of the insulating and non-magnetic matrix phase, these materials have a distributed air gap that limits their $\mu_r$ to a range of 100 to 500. However, the insulating matrix also boosts their $\rho$ ($10^{-3}$ to $10^{-1}$ μohm·m), reducing eddy current losses. SMCs can also be pressed into more complex final geometries without the need of any machining (net-shaping), which can substantially reduce manufacturing costs. Their isotropic nature, low cost, and the ability to net-shape complex parts have made SMCs fairly successful in rotating electrical machines (*32, 33*).

The brief history of soft magnetic materials described above (which is summarized graphically in Fig. 3) is by no means exhaustive. Instead, our intent is to focus on materials that have been and will continue to be competitive for the fabrication of soft magnetic components in high-frequency power electronics and electrical machines. Performance metrics such as $M_s$ and core loss are extremely important. However, because soft magnetic parts will need to be used in large quantities, the importance of cost cannot be neglected. For this reason, soft ferrites still remain a competitive core material at high frequency. Because of their excellent performance at high frequency, the amorphous and nanocrystalline alloys will certainly continue to be key materials. Although silicon steels still make up a majority of the global market for soft magnetic materials, their primary applications are in large transformers operating at 50 or 60 Hz and slow rotational speed electrical machines. Thus, we will not discuss silicon steel further. We will also consider new soft magnetic materials being developed, which include both top down and bottom up approaches that could build upon a foundation of work established in the area of SMCs.

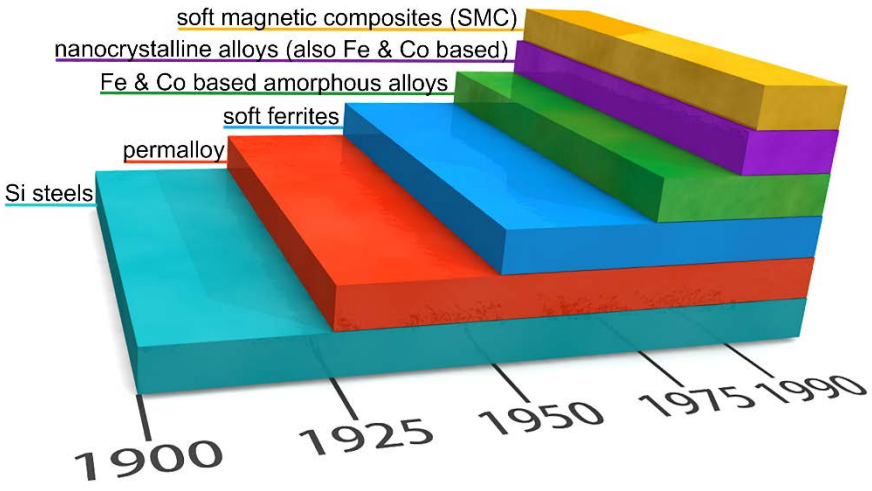


**Fig. 3. A brief history of soft magnetic materials.** A synopsis of the progression of soft magnetic materials. The chart is by no means exhaustive. [Modified from (*34*), with permission]

## Soft ferrites

Ferrites are distinctive soft magnetic materials in that they are ionic compounds. They are also ferrimagnetic, whereas all of the other soft magnetic materials are ferromagnetic. J. L. Snoek and his co-workers developed ferrites between 1933 and 1945 at the Philips Research Laboratories in Eindhoven, Netherlands where commercial cores were required for Pupin coils in telephone cables and loudspeakers (*28*). They investigated the properties of magnetic oxides of the chemical formula $MO{\cdot}Fe_2O_3$, where M is a divalent ion (such as $Fe^{2+}$, $Mn^{2+}$, $Ni^{2+}$, $Zn^{2+}$, and $Mg^{2+}$) known to occupy two different kinds of crystallographic positions (A and B sites) within the oxide cell. L. Néel made the basic assumption that the exchange force acting between ions on the A and B sites was negative, providing the theoretical key to an understanding of the phenomena of ferrimagnetism and antiferromagnetism in ferrites, where magnetization is caused by the magnetic moments of the metal ions, but not according to the conventional ferromagnetic exchange interaction (*35*).

The commercial production of these metal oxides is typically achieved with ceramic processing, starting with either the calcination of iron salts, base oxides, or metal carbonates. The starting reagents are thoroughly mixed by prolonged wet grinding until a homogeneous fine powder is obtained with granule dimensions in the micrometer range. Additional calcining and grinding steps may be applied at this point. Finally, the powders are mixed with a binder, pressed at high pressures and then sintered at temperatures up to 1400°C in a controlled atmosphere. The final product, hard and brittle, is a semiconductor with an electrical resistivity six orders of magnitude higher than in Fe-based metallic alloys. Thus, even when a rapidly changing magnetic field is applied, eddy currents and energy loss are contained. This property

makes ferrites suitable for high frequency applications and they currently are the most extensively used magnetic material up to few hundred megahertz.

Figure 4 shows one-eighth of single unit of the cubic spinel (named after the mineral spinel, $MgO \cdot Al_2O_3$) ferrite structure: the metallic cations are separated by the oxygen anions ($O^{2-}$) arranged in a face-centered cubic (fcc) structure; the small metal ions occupy interstitial positions, at either tetrahedral (A) or octahedral (B) sites, surrounded by four or six oxygen ions, respectively. Direct exchange interaction between the 3d electron spins of the metallic cations is negligible whereas an indirect coupling mechanism, superexchange, occurs. The superexchange interaction is stronger when a straight line connects the cations through the $O^{2-}$ ion (*36*). The A-B coupling, which is associated with an A-O-B angle around 125°, is much stronger than the A-A and B-B couplings through oxygen, whose angles are 90° and 80°, respectively. It involves the spins of the two extra 2p electrons in the $O^{2-}$, which interact with the 3d spins of the two neighboring metal cations. The mediating effect of the oppositely directed oxygen spins is such that the A and B ions' total magnetic moments are bound, according to Hund's rule, to antiparallel directions.

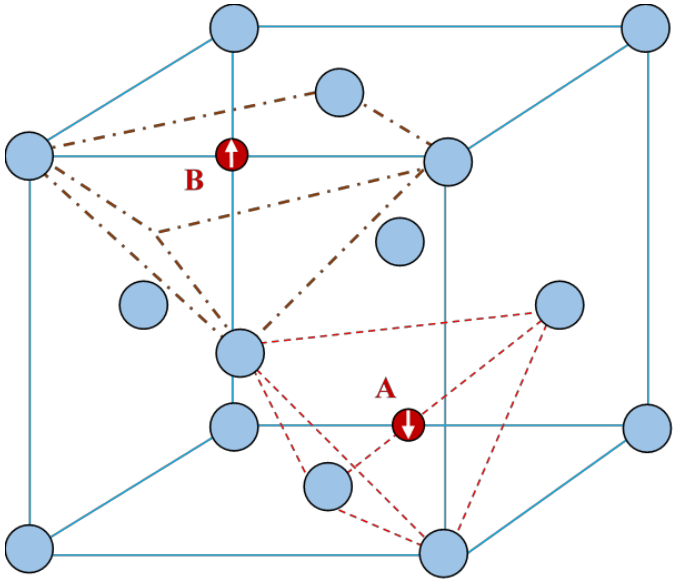


**Fig. 4. One-eighth portion of the unit cell of a cubic spinel ferrite (ferrospinel).** The $O^{2-}$ ions (cyan) arrange in a fcc lattice. The metal ions (red) arrange either in tetrahedral (A) or octahedral (B) interstitial sites, having ferrimagnetic (unbalanced antiferromagnetic) spin. The AB coupling mediated by the oxygen ion leads to antiparallel configuration of metallic spins in tetrahedral and octahedral sites. [Modified from (*2*), with permission]

Ferrites have an antiferromagnetic configuration of the two sublattices corresponding with A ions spontaneously magnetized in one direction, and B ions magnetized in the opposite direction. When the magnitudes of A and B spins are not equal, the material becomes a ferrimagnet and a net spontaneous magnetization results. The distribution of the divalent ions on A and B sites (and thus the magnetic properties) can be further modified by heat treatment; it may depend on whether the material is quenched from a high temperature or slowly cooled. The

ferrimagnetic nature of ferrites results in a relatively low $M_s$, typically 0.4 MA/m or less at room temperature. In addition, $M_s$ in ferrites is more temperature-sensitive than in ferromagnetic materials(*2, 3, 22*).

Ferrites can contain two or more different divalent ions, producing a mixed ferrite. The most common commercial soft ferrites have mixed cations, (Ni, Zn)O·$Fe_2O_3$, and (Mn, Zn)O·$Fe_2O_3$, but suppliers do not typically share the exact composition of their ferrites and instead provide performance specifications. In an interesting interplay between the ions within the spinel structure, the addition of nonmagnetic (*37*) ZnO·$Fe_2O_3$ to mixed ferrites actually increases their $M_s$. The presence of two or more metal ions $M^{2+}$ provides great versatility of the magnetic properties. By making suitable additions and thermal treatments, material tailoring to specific applications can be achieved. For example, the mixed ferrites display a cubic symmetry with negative value of the anisotropy constant, K. By adjusting composition and processing, very low anisotropy (and therefore low $H_c$) can be obtained over a range of temperatures suitable for many applications (20–100°C). Additionally, the temperature stability of $\mu_r$ can be controlled also by the addition of $M^{2+}$ ions, like $Fe^{2+}$ or $Co^{2+}$. The highest $\mu_r$ of ferrospinels are found in the Mn–Zn ferrites, whereas Ni–Zn ferrites have a much higher $\rho$, depending on the amount of doping with $Fe^{2+}$ (*38*).

The near-insulating character of ferrites is conducive to a nearly constant value of $\mu_r$ over many frequency decades, typically up to the MHz region in Mn–Zn ferrites ($\rho$ = 10–$10^4$ μohm·m) and the 10-MHz region in Ni–Zn ferrites ($\rho$ as high as $10^8$ μohm·m). This is illustrated in Fig. 5A, where the behavior vs. frequency of the real component ($\mu'$) of the relative initial permeability is presented for a commercial Mn–Zn ferrite at a peak polarization, $J_p$, ranging between 2 and 300 mT. The rather sudden drop in $\mu'$ is brought on by the onset of electron spin resonance and is matched by a prominent peak in the imaginary permeability ($\mu''$). See Fig. 5B for a plot of $\mu''$ for values of $J_p$ ranging between 2 and 300 mT. This response cannot be observed in other soft magnets because of their much lower $\rho$.

For application in the microwave region ($f$ = 0.5 – 100 GHz), larger magnetic anisotropies are required. In this high-$f$ range, a technical limitation was stated by Snoek (*39*) in 1948. Snoek observed that the product of DC initial susceptibility, $\chi_i$, and resonance frequency, $f_0$, is a constant value related to spin precession and thus the magnetocrystalline anisotropy, K. In a bulk polycrystalline material, Snoek's law is written as

$$\chi_i f_0 = (1/2\pi)\gamma\mu_0 M_s \qquad (5)$$

where $f_0$ is the critical (resonance) frequency, $\chi_i$ the low frequency susceptibility, $\gamma$ the gyromagnetic ratio, and $M_s$ the saturation magnetization. Experimentally, the critical frequency may be taken as that at which the imaginary susceptibility $\chi''$ peaks (see Fig. 5.B).

Some ferrites, such as Ba *M*-type (BaM) ferrites, having the same hexagonal structure of magnetoplumbite $BaO(Fe_2O_6)_3$, consist of spinel blocks rotated 180° with respect to one another

and separated by an atomic plane containing the Ba atoms. This plane breaks the crystal symmetry and results in a hexagonal structure with a high K – shifting Snoek's limit up to 36 GHz. The large K of BaM ferrites can be combined with growth on substrates that introduce a high degree of crystal texture, such as MgO layers deposited on single crystalline SiC (*40*), allowing the use of hexagonal ferrites in a variety of microwave devices.

With their high ρ, constant $\mu_r$ that extends well into the MHz frequency range, and low cost, ferrites will continue to play a role in applications where only low values of $J_p$ (and low energy density) are required. Although ferrites have been around for a long time, strategies to improve their performance including grain boundary engineering (*41*) and embedding them in substrate materials (*42*) are being considered.

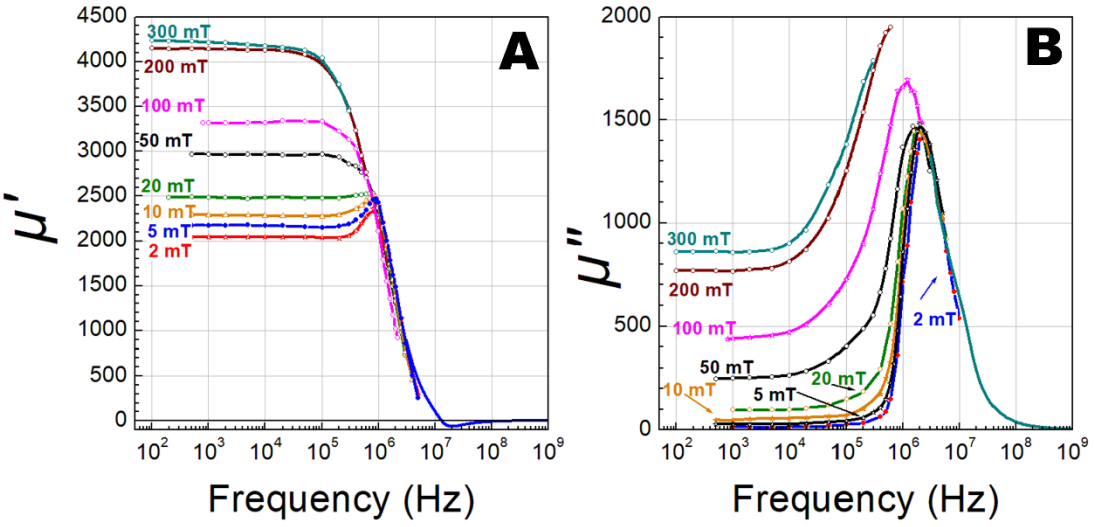


**Fig. 5. Soft ferrite permeability response.** Measurements of (**A**) the real part (μ′) and (**B**) the imaginary part (μ″) of permeability vs. frequency for a commercial (N87) Mn-Zn ferrite at peak magnetic polarizations, $J_p$, ranging from 2 to 300 mT. Permeability curves tend to coalesce above $f \sim 1$ MHz, where relaxation of the domain wall displacements is completed and only spin rotation processes survive. [courtesy of F. Fiorillo, C. Beatrice, and S. Dobák]

## Amorphous and nanocrystalline alloys

In 1967, Duwez and Liz reported the first amorphous soft magnetic alloy in the form of small disk-shaped samples. They used a rapid solidification technique called splat cooling of the Fe–P–C system (*29*). Alloy composition engineering and the development of planar flow casting led to the production of amorphous ribbons from 5 to 50 μm in thickness and up to 10 inches (25.4 cm) in width (see Fig. 6). Rapid cooling rates of $10^6$°C/s freeze the alloy into an amorphous structure. As reported by Yoshizawa et al. in 1988, optimized compositions allow partial devitrification of the metallic glass during a controlled heat treatment. This process results

in a nanocrystalline soft magnetic material that consists of ~ 10 nm diameter ferromagnetic nanograins embedded in an amorphous matrix (i.e. glass ceramic) (*30*). Alben *et al*. explained that when the magnetic correlation length is longer that the structural correlation length, as in amorphous ferromagnetic materials, the effective magnetocrystalline anisotropy becomes negligible (*43*). This random anisotropy model was later extended to nanocrystalline materials by Herzer (*44*, *45*). Given the relatively high ρ of both amorphous and nanocrystalline alloys relative to crystalline materials and their very thin laminations, eddy current losses in these materials are very low and they can operate safely into the tens of kilohertz frequency range (*46*). It should be pointed out that multi-phase resistivity models are necessary to understand the compositional dependence on the ρ in nanocrystalline materials (*47*).

**Fig. 6. Ribbon of amorphous soft magnetic alloy.** Thin (5 to 50 μm) ribbons of amorphous alloys are produced by planar flow casting.

FINEMET was the first family of nanocrystalline alloys to be commercialized. Its most common composition is $Fe_{73.5}Si_{13.5}B_9Nb_3Cu_1$ (*30*), which is based on the amorphous Fe–Si–B system, where Si and B enhance glass formation. During the devitrification process, Cu favors the nucleation of segregated Fe–Si crystals, whereas the large Nb atoms control grain growth and prevent the crystallization of anisotropic boride phases. The composite structure of FINEMET–type alloys has another strength: Fe–Si nanocrystals have a negative magnetostriction that balances the positive magnetostriction of the amorphous matrix, diminishing stress anisotropy ($K_\sigma$). The combination of vanishing magnetocrystalline and stress anisotropies results in a very low $H_c$ (under 10 A/m) and a very high initial $\mu_r$ ($10^4$ to $10^6$). $M_s$ ranges from about 0.9 to 1.0 MA/m. Unfortunately, nanocrystalline Fe-based alloys are extremely brittle. Thus, they must be annealed in the final core geometry and be handled carefully.

Because of their attractive characteristics, amorphous and nanocrystalline soft magnetic materials became a research focus in the years following their invention (*48*). The addition of

Co to develop FeCo–based alloys (*49*) served two purposes. First, it increases $M_s$ to 1.0 to 1.2 MA/m. Second, Co increases the Curie temperature of the amorphous and crystalline phases and allows higher operating temperatures. However, the increased magnetostriction of FeCo–based alloys makes them sensitive to manufacturing processes, such as impregnation and cutting. When the iron is removed, pure Co–based alloys exhibit reduced $M_s$ (0.6 to 0.8 MA/m) but are also suitable for high-temperature applications. Their composition can be tuned to exhibit near zero magnetostriction or to enhance responses to anisotropic magnetic and stress fields during annealing, achieving $\mu_r$ values from 10 to $10^4$ as needed for a given application (*50*). These cobalt-rich alloys can also have a dramatically improved ductility, even in the nanocrystalline state. Additionally, the modification of glass-former content in amorphous and nanocrystalline alloys has led to the optimization of other characteristics such as corrosion (*51, 52*) and oxidation resistance (*53*), raw materials costs (*54*), and $M_s$ (up to 1.5 MA/m (*55, 56*)).

All families of amorphous and nanocrystalline materials have a common disadvantage: they are mechanically very hard [typically 800 to 1000 Vickers hardness (HV)], making machining a difficult and expensive task. If a conventional stamping process were used, dies would wear out quickly. These fabrication issues have held back their application in complex geometries for electric machines.

The first attempts to use amorphous materials for electric motors date back to 1981, just after the 1970s energy crisis. Mischler *et al*. demonstrated the low loss potential of the amorphous stator, but the fabrication technique required improvement (*57*). Since then, industry and academia have devoted their efforts to improving the fabrication of electric motors using amorphous and nanocrystalline soft magnetic materials. Given that either stacking or winding amorphous ribbons yield similar losses (*58*), researchers have applied both approaches in combination with cutting and machining. Additional methods have been used to cut mechanically hard amorphous sheets including chemical etching (*59*), wire EDM (electric discharge machining), and laser cutting (*60*). Laser cutting, however, has been shown to overheat and deteriorate the edges of Fe-rich amorphous materials (*61*). Grinding, EDM (*62, 63*), or waterjet (*64*) cutting have also been used to machine already assembled ribbons into the final core geometry, speeding up the manufacturing process.

When manufacturing challenges can be overcome, losses can be substantially reduced. An example is shown in Fig. 7 where finite-element analysis was used to calculate the distribution of losses in motor stators fabricated with silicon steel and Co–rich amorphous alloy. Axial motors can be particularly suited for amorphous laminations, as demonstrated by Hitachi with a 11-kW prototype motor that achieved an efficiency greater than that of the IE5 efficiency class for induction motors (*65*). Recently, some groups have also demonstrated the feasibility of constructing highly efficient electric motors with nanocrystalline cores (*66, 67*).

Amorphous core transformers have been commercially available since the 1980s. A decade later, 6 to 8% of the distribution transformers bought in the U.S. were built with

amorphous cores (*68*). With manufacturing plants in Japan and in the U.S., Hitachi Metals Ltd, has currently a global production capacity of 100,000 tons per year and dominates this market. The U.S. Department of Energy revealed that in the long term, amorphous cores are likely to predominate in the transformer market because of their higher efficiency (*69*). Asia, for example, has widely adopted amorphous core distribution transformers for the reduction of electrical grid losses. By the end of 2010, the total capacity of these transformers had reached 70 million kVA in China and 35 million kVA in India (*70*). Meanwhile, the worldwide production rate of nanocrystalline materials has exceeded 1,000 tons per year, and continues to increase (*48*). Researchers are also continually working to improve the performance of both amorphous and nanocrystalline alloys, seeking to boost $M_s$ in particular (*71*).

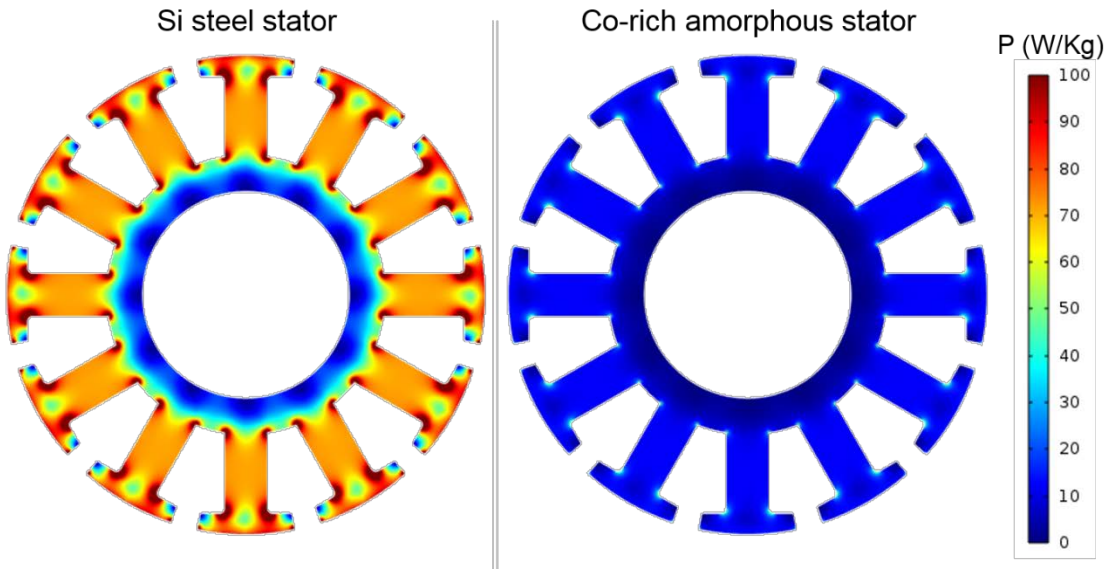


**Fig. 7. Motor stator power loss (P).** Distribution of power loss (P) in a motor stator fabricated using silicon steel (left) and Co-rich amorphous alloy (right). The motor speed was 18,000 rpm (f = 2.1 kHz). [ From (*61*)]

## Soft magnetic composites

During the past three decades, most of the effort in magnetic composites has focused on the development of powder cores, which are also referred to as soft magnetic composites (SMCs). SMCs have been constructed of micrometer-scale particles (most often comprised of Fe but sometimes consisting of alloys such as MPP, Fe–P, Fe–Si, or Fe–Co) while only very recently have magnetic composites begun taking advantage of nanoparticles. To date, there are no commercially available soft magnetic cores that take advantage of nanoparticles. However, the previous work in SMCs has paved the way for the introduction of nanoparticle-based magnetic composites.

The advantages of composite magnetic cores generally take the form of reduced energy losses during magnetic cycling, which can be strongly effected by composite structure (*31*). By embedding the conductive magnetic particles in an insulating matrix, composites increase $\rho$ ($10^{-3}$ – $10^{-1}$ $\mu$ohm·m) and reduce eddy current losses (*72*), although magnetic hysteresis losses systematically increase (*73*). This increase in $H_c$ is caused by the retention of mechanical stresses in both mechanically milled and chemically synthesized particles (*31*). Although a high-temperature anneal could relieve many of these stresses, it would lead to decomposition of the organic binder. This is one area where transitioning to nanometer-sized particles could benefit composites, as it is much easier to anneal away defects and stresses in nanoparticles (*74*).

Magnetic composites also yield an opportunity to tune the $\mu_r$, and in turn the saturation behavior, of the material. In almost all cases, saturation of the magnetic core during operation is highly undesirable. Traditional designs avoid saturation by limiting the applied current, reducing the number of windings, increasing the core size, or introducing an air gap in the magnetic core to reduce $\mu_r$. Similar to gapped cores, spacings of non-magnetic material in the direction of magnetization can be considered a distributed air gap. A distributed gap avoids the magnetic flux leakage that occurs in a core with a discrete air gap. The gaps in a composite material are exceedingly small due to their large number, and so only a negligible magnetic flux extends beyond the core. A composite (whether micrometer or nanoscale) magnetic core can be viewed as a distributed air gap inductor with 10 to $10^8$ air gaps per cm, depending upon the dimensions of the magnetic particulate. In addition to increasing the saturation field, a distributed air gap promotes soft saturation. This condition leads to a slow decrease in $\mu_r$ as saturation is approached, making for a less precipitous and disruptive saturation.

Some additional advantages of composite magnetic materials come from added flexibility in manufacturing. Composite materials can be formed with the application of relatively mild forces and low temperatures. For example, an iron powder SMC core is typically made with mild compaction and moderate heating, generally less than 200°C for organic matrices (*75*), and around 500°C for inorganic matrices (*72*). This processing is also amenable to net-shaping, allowing for complex shapes to be produced directly during the compaction stage and without the need for additional machining. Composites also suppress eddy currents isotropically in all directions, leading to additional freedom in the design of systems (*31*).

There is an opportunity to further increase the performance of magnetic composites by transitioning to nanoparticle-based magnetic materials. However, at this point, there have been very few published reports in this area. Transitioning from micrometer- to nanoscale particles can leverage decades of continuous study of isolated magnetic nanoparticles (*76*). Fig. 8 illustrates some of the differences between composites fabricated using micrometer-sized particles and nanoparticles. In some respects, nanocomposites are a continuation of trends noted for larger scale materials. For example, through the reduction of particle size, eddy current losses can be reduced to the point of being negligible. However, the reduction of particle size also introduces new physics.

Hysteresis losses have a complex relation to particle size. At bulk sizes, soft magnetic materials have modest hysteretic losses, but as their size decreases, the stresses and surface defects present in micrometer-scale materials enhance the hysteresis. Further decreases in scale that approach the characteristic magnetic domain size of a magnetic material lead to a maximum in hysteresis.(*77*) Single domain particles do not reverse their magnetization by domain wall motion, but through rotation of the magnetic moments within each particle. The energy required for this rotation in the largest single domain particles is very high. However, this energy decreases linearly with number of electron spins, and therefore as $r^3$ (where r is the particle radius). When the nanoparticles reach a critical size, generally in the tens of nanometers, the thermal energy present in a system provides enough energy to freely reorient the magnetization direction of the particle (*78*). The temperature above which this is true is the superparamagnetic blocking temperature ($T_B$). These particles no longer exhibit magnetic hysteresis, and are referred to as superparamagnetic, as the equations that govern paramagnetism can also be applied though with a much larger number of electron spins (*79*). The elimination of $H_c$ is coupled with the ability to achieve very high values of $\mu_r$.

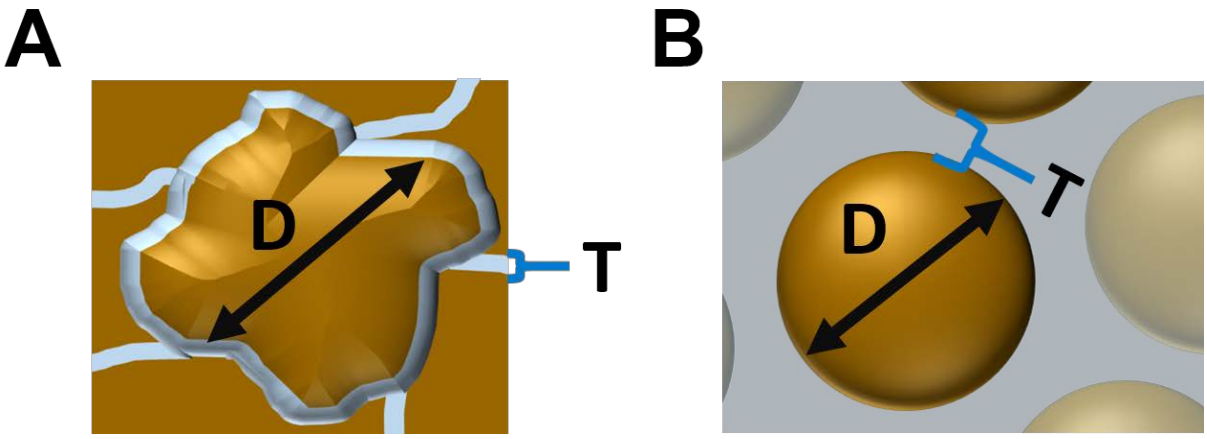


**Fig. 8. Magnetic composites.** (**A**) Micrometer-scale composites are highly compressed to yield a dense material, typically with irregularly shaped particles. Increasing the particle effective diameter (D) tends to increase $M_s$ and $\chi$, while also increasing eddy current losses. As the thickness (T) of the dielectric layer increases, eddy current losses tend to decrease, as do $M_s$ and $\chi$. (**B**) Nanocomposites tend to retain their initial particle shapes and have few defects or residual stress. The interplay between particle diameter (D), spacing (T), $M_s$, and $\chi$ are more complex than in micrometer-scale composites (see discussion in text) but offer the opportunity for more precise tuning of magnetic response. Eddy current losses can become negligible in a well-designed nanocomposite because of the small size of the electrically isolated particles.

The weakness of superparamagnetic nanocomposites is the appreciable volume that must be dedicated to the nonmagnetic matrix isolating the individual nanoparticles. If magnetic nanoparticles come into close contact, the particles can magnetically couple and form ferromagnetic domains, leading to domain walls and magnetic hysteresis. While SMCs with micrometer-sized particles can have very high volumetric loading of magnetic material, it is hard

to conceive of a superparamagnetic nanocomposite with much higher than 50% magnetic material.

Although the details of optimization will be complex, by controlling nanoparticle size and spacing, a superparamagnetic nanocomposite can be optimized for use at a specific temperature and frequency. The result would be a material of exquisitely low loss, with a magnetization that, while lower than that of other magnetic composites, is optimum for a nanocomposite. Because of the complexity of this approach, optimized systems have not been reported to date, though some experiments are beginning to approach this level of control (*80*) and at least one optimization system has been proposed (*81*).

## Conclusions and Outlook

Soft magnetic materials have been advancing since the days of Faraday, although more in a series of bursts than a steady progression. The introduction of WBG semiconductors and new power electronics leveraging them has left the magnetic materials community with a daunting challenge. WBG devices are also finding their way into faster controllers for electric machines, setting the stage for high rotational speeds and increased efficiency if the development of advanced, high performance soft magnets can keep up. Many in the research community are now awakening to the need to push research in soft magnetic materials onward with greater urgency.

There are promising magnetic materials that can work at the higher frequencies required in modern power electronics and electrical machines that have been covered in this review. As mentioned earlier, our coverage was not exhaustive but intended to highlight the most promising materials for a majority of the high frequency applications. There is no single soft magnetic material that can satisfy the needs of all power electronic and electrical machine applications. Instead, designers will need to choose judiciously from the available materials, with cost being weighed alongside performance metrics.

Despite being a relatively old material, soft ferrites continue to be an excellent choice in applications where high power densities are not required. As insulators, they are one of the best materials for mitigating losses and they are extremely affordable. Even though ferrites have been around since the 1940s there are still opportunities for improvement through grain boundary engineering and new processing approaches. Today, amorphous and nanocrystalline alloys are the current state of the art materials. Their distinctive nanostructure coupled with extremely thin laminations keep losses very low, while still preserving respectable values of $M_s$. And researchers continue to steadily improve the $M_s$ of nanocrystalline and amorphous alloys even further. However, the specialized processing required to produce tapes of these materials keeps their cost high. The thin, brittle laminations can also make fabrication of parts challenging.

Technical issues are not the only barrier limiting the adoption of amorphous and nanocrystalline materials to high-end niche applications. Many large and costly electrical machines and transformers still have a long remaining lifetime. Higher up-front costs raise the CapEx–to–OpEx ratio (Capital Expenditures/Operating Expenses), but also status quo bias and lack of information affect decision-making. Soft magnetic composites are proving useful as a relatively low-cost material in rotating electrical machines, due to their isotropic nature. There is hope for much higher performance SMCs, making eddy current and hysteresis losses negligible, by transitioning from micrometer- to nanometer-sized particles. Nanocomposites could also open the door for three-dimensional printing and microfabrication of inductive components, but work on magnetic nanocomposites is only in its initial stages.

The development of entirely new materials and composites is certainly a possibility, particularly as more in the scientific community awaken to the need for advanced magnetic materials to pair with new WBG devices. It will be necessary to improve control over the nanostructure of both existing and emerging materials in order to lessen barriers to magnetization reversal. Nanostructure optimization and grain boundary engineering can also further mitigate eddy current losses. Optimization of the structure within magnetic materials will require increased use of advanced characterization tools.

These will include techniques applied to almost all materials such as electron microscopy and x-ray (including synchrotron-based) characterization. Techniques specific to imaging magnetic domain structure, such as Lorentz microscopy (*82*), electron holography (*83*), magnetic force microscopy (MFM) (*84*), x-ray magnetic circular dichroism (XMCD) spectroscopy(*85*), and imaging based on the magneto-optical Kerr effect (MOKE) (*1, 86*) will be particularly helpful. It is now up to the community of materials scientists, physicists, chemists, and others to apply these techniques and our knowledge of magnetic materials to meet the demands of the next generation of power electronics and electrical machines.

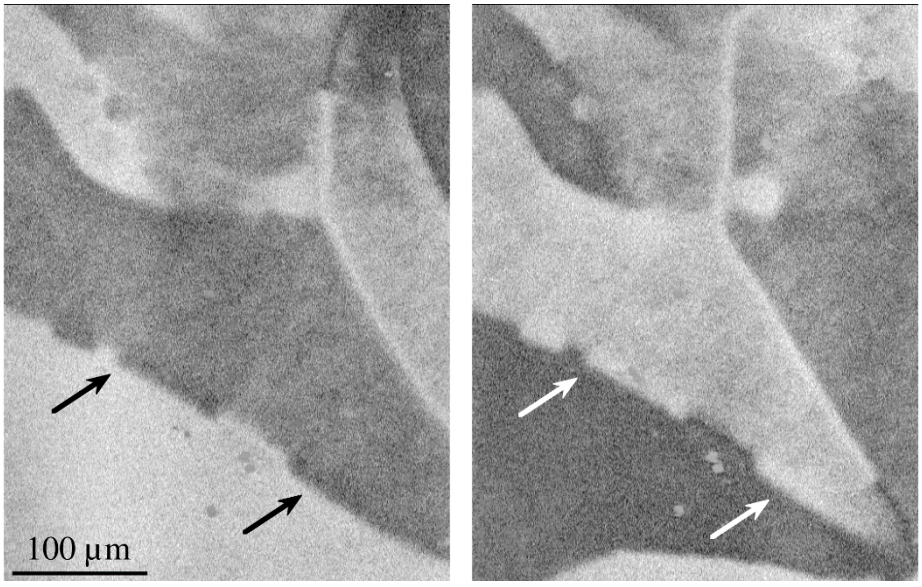

**Fig. 2. Pinned domain wall.** A pinned domain wall in an amorphous alloy ribbon is marked by arrows in both the left and right Kerr microscopy image. The position of the pinned wall remains fixed while the surrounding domain structure changes from left to right. [From (*1*)]

## Acknowledgements

JMS acknowledges support from CONICET and UBACyT 20020150200168BA. EF would like to acknowledge his colleague Fausto Fiorillo, for his continuous support and fruitful suggestions. TCM and DLH were funded in part by Sandia's Laboratory Directed Research and Development program. TCM acknowledges partial support from the Energy Storage program of the U.S. Department of Energy, Office of Electricity Delivery and Energy Reliability and thanks Dr. Imre Gyuk, Director of the Energy Storage program. DLH acknowledges partial support from the Center for Integrated Nanotechnologies, an Office of Science User Facility operated for the U.S. Department of Energy (DOE) Office of Science. Sandia National Laboratories is a multimission laboratory managed and operated by National Technology and Engineering Solutions of Sandia LLC, a wholly owned subsidiary of Honeywell International Inc. for the U.S. Department of Energy's National Nuclear Security Administration under contract DE-NA0003525.

1. R. Schaefer, G. Herzer, Continuous magnetization patterns in amorphous ribbons. *IEEE Transactions on Magnetics* **37**, 2245-2247 (2001).
2. F. Fiorillo, G. Bertotti, C. Appino, M. Pasquale, in *Wiley Encyclopaedia of Electrical and Electronics Engineering*, J. G. Webster, Ed. (2016), doi:10.1002/047134608X.W4504.pub2.
3. F. Fiorillo, *Measurement and Characterization of Magnetic Materials*. (Elsevier, Amsterdam, 2004)
4. H. J. Williams, W. Shockley, C. Kittel, Studies of the Propagation Velocity of a Ferromagnetic Domain Boundary. *Physical Review* **80**, 1090-1094 (1950).
5. R. H. Pry, C. P. Bean, Calculation of the Energy Loss in Magnetic Sheet Materials Using a Domain Model. *Journal of Applied Physics* **29**, 532-533 (1958).
6. G. Bertotti, *Hysteresis in Magnetism*. (Academic Press, San Diego, CA 1998)
7. S. Flohrer *et al.*, Dynamic magnetization process of nanocrystalline tape wound cores with transverse field-induced anisotropy. *Acta Materialia* **54**, 4693-4698 (2006).
8. G. Bertotti, Physical interpretation of eddy current losses in ferromagnetic materials. I. Theoretical considerations. *Journal of Applied Physics* **57**, 2110-2117 (1985).
9. G. Bertotti, General properties of power losses in soft ferromagnetic materials. *IEEE Transactions on Magnetics* **24**, 621-630 (1988).
10. F. Fiorillo, Measurements of magnetic materials. *Metrologia* **47**, S114–S142 (2010).
11. F. Fiorillo, E. Ferrara, M. Coïsson, C. Beatrice, N. Banu, Magnetic properties of soft ferrites and amorphous ribbons up to radiofrequencies. *J. Magn. Magn. Mater.* **322**, 1497–1504 (2010).
12. F. Fiorillo, C. Appino, M. Pasquale, in *The Science of Hysteresis Vol. II*, G. Bertotti, I. Mayergoyz, Eds. (Academic Press, 2006), pp. 1-189.
13. F. F. A. Magni, E. Ferrara, A. Caprile, O. Bottauscio, C. Beatrice, Domain wall processes, rotations, and high-frequency losses in thin laminations. *IEEE Trans. Magn* **48** 3796–3799 (2012).
14. S. Bhattacharya, Transforming the transformer. *IEEE Spectrum* **54**, 38-43 (2017).
15. S. Krishnamurthy, in *2012 Twenty-Seventh Annual IEEE Applied Power Electronics Conference and Exposition (APEC)*. (2012), pp. 1414-1417.
16. J. W. Kolar, J. Biela, S. Waffler, T. Friedli, U. Badstuebner, in *2010 6th International Conference on Integrated Power Electronics Systems*. (2010), pp. 1-20.
17. P. Waide, C. U. Brunner, "Energy-efficiency policy opportunities for electric motor-driven systems," *Working paper of the International Energy Agency (IEA)* (2011); https://www.iea.org/publications/freepublications/publication/EE_for_ElectricSystems.pdf.
18. A. Krings, A. Boglietti, A. Cavagnino, S. Sprague, Soft magnetic material status and trends in electric machines. *IEEE Transactions on Industrial Electronics* **64**, 2405-2414 (2017).
19. G. A. McCoy, T. Litman, J. G. Douglass, "Energy-efficient electric motor selection handbook," (1990); https://www.osti.gov/scitech/servlets/purl/6116458.
20. A. Krings, Doctoral Dissertation, KTH, Stockholm (2014).

21. J. M. Silveyra, A. Leary, V. DeGeorge, S. Simizu, M. McHenry, High speed electric motors based on high performance novel soft magnets. *Journal of Applied Physics* **115**, 17A319 (2014).
22. B. D. Cullity, C. D. Graham, *Introduction to Magnetic Materials*. (IEEE Press, Piscataway, New Jersey, 2nd ed., 2009)
23. "Super Core™ Electrical steel sheets for high-frequency application," JFE Steel Corporation, (2017); http://www.jfe-steel.co.jp/en/products/electrical/catalog/f1e-002.pdf.
24. K. Shoji, N. Misao, H. Tatsuhiko, "Recent Progress of High Silicon Electrical Steel in JFE Steel," (JFE Steel Corporation, 2016); http://www.jfe-steel.co.jp/en/research/report/021/pdf/021-04.pdf.
25. H. D. Arnold, G. W. Elmen, Permalloy, A New Magnetic Material of Very High Permeability. *Bell System Technical Journal* **2**, 101-111 (1923).
26. A. Alabakhshizadeh, O. M. Midtgård, K. Boysen, in *2013 IEEE 39th Photovoltaic Specialists Conference (PVSC)*. (2013), pp. 2845-2848.
27. "MPP Cores," Magnetics®, https://www.mag-inc.com/Products/Powder-Cores/MPP-Cores
28. M. J. de Vries, *80 Years of Research at the Philips Natuurkundig Laboratorium (1914-1994). The Role of the Nat. Lab. at Philips*. (Amsterdam University Press, Amsterdam, 2005)
29. P. Duwez, S. C. H. Lin, Amorphous ferromagnetic phase in iron-carbon-phosphorus alloys. *Journal of Applied Physics* **38**, 4096-4097 (1967).
30. Y. Yoshizawa, S. Oguma, K. Yamauchi, New Fe-based soft magnetic alloys composed of ultrafine grain structure. *Journal of Applied Physics* **64**, 6044-6046 (1988).
31. H. Shokrollahi, K. Janghorban, Soft magnetic composite materials (SMCs). *Journal of Materials Processing Technology* **189**, 1-12 (2007).
32. A. G. Jack *et al.*, Permanent-magnet machines with powdered iron cores and prepressed windings. *IEEE Transactions on Industry Applications* **36**, 1077-1084 (2000).
33. L. O. Hultman, A. G. Jack, in *Electric Machines and Drives Conference, 2003. IEMDC'03. IEEE International*. (2003), vol. 1, pp. 516-522 vol.511.
34. L. Dobrzański, M. Drak, B. Ziębowicz, Materials with specific magnetic properties. *Journal of Achievements in Materials and Manufacturing Engineering* **17**, 37-40 (2006).
35. L. Néel, Propriétés magnétiques des ferrites : ferrimagnétisme et antiferromagnétisme. *Ann. Phys* **3**, 137-198 (1948).
36. P. W. Anderson, Antiferromagnetism. Theory of Superexchange Interaction. *Phys. Rev* **79**, 350-356 (1950).
37. All materials have a magnetic moment and can be described as diamagnetic, paramagnetic, ferromagnetic, etc. Since diamagnetic and paramagnetic materials are so weakly magnetic that their contribution to a ferromagnetic or ferrimagnetic material can be ignored, they will be referred to as nonmagnetic for simplicity.
38. L. K. V. F. Mazaleyrat, Ferromagnetic composites. *J. Magn. Magn. Mater.* **215–216**, 253–259 (2000).
39. J. L. Snoek, Dispersion and absorption in magnetic ferrites at frequencies above one Mc/s. *Physica* **14**, 207-217 (1948).

40. P. R. Ohodnicki *et al.*, Correlation between texture, anisotropy, and vector magnetization processes investigated by two-dimensional vector vibrating sample magnetometry in BaO(Fe2O3)6 thin film. *Journal of Applied Physics* **103**, 07E514 (2008).
41. Y. Chen, V. G. Harris, U.S. patent 9,117,565, Magnetic grain boundary engineered ferrite core materials, 2015
42. A. W. Roesler *et al.*, Planar LTCC Transformers for High-Voltage Flyback Converters. *IEEE Transactions on Components and Packaging Technologies* **33**, 359-372 (2010).
43. R. Alben, J. Becker, M. Chi, Random anisotropy in amorphous ferromagnets. *Journal of Applied Physics* **49**, 1653-1658 (1978).
44. G. Herzer, Grain structure and magnetism of nanocrystalline ferromagnets. *IEEE Transactions on Magnetics* **25**, 3327-3329 (1989).
45. G. Herzer, in *Handbook of magnetism and advanced magnetic materials*. (John Wiley and Sons, 2007).
46. A. M. Leary, P. R. Ohodnicki, M. E. McHenry, Soft magnetic materials in high-frequency, high-power conversion applications. *JOM Journal of the Minerals, Metals and Materials Society* **64**, 772-781 (2012).
47. V. DeGeorge, S. Shen, P. Ohodnicki, M. Andio, M. E. McHenry, Multiphase Resistivity Model for Magnetic Nanocomposites Developed for High Frequency, High Power Transformation. *Journal of Electronic Materials* **43**, 96-108 (2014).
48. G. Herzer, Modern soft magnets: Amorphous and nanocrystalline materials. *Acta Materialia* **61**, 718-734 (2013).
49. M. Willard *et al.*, Structure and magnetic properties of (Fe 0.5 Co 0.5) 88 Zr 7 B 4 Cu 1 nanocrystalline alloys. *Journal of Applied Physics* **84**, 6773-6777 (1998).
50. A. Leary *et al.*, Stress induced anisotropy in Co-rich magnetic nanocomposites for inductive applications. *Journal of Materials Research* **31**, 3089-3107 (2016).
51. J. May, C. A. C. d. Souza, C. Morelli, N. Mariano, S. E. Kuri, Magnetic and corrosion properties comparison of FeSi-based, FeZr-based and FeCo-based alloys. *Journal of Alloys and Compounds* **390**, 106-111 (2005).
52. C. Souza, D. Ribeiro, C. Kiminami, Corrosion resistance of Fe-Cr-based amorphous alloys: An overview. *Journal of Non-Crystalline Solids* **442**, 56-66 (2016).
53. J. M. Silveyra, E. Illeková, Effects of air annealing on Fe–Si–B–M–Cu (M= Nb, Mo) alloys. *Journal of Alloys and Compounds* **610**, 180-183 (2014).
54. J. M. Silveyra *et al.*, High performance of low cost soft magnetic materials. *Bulletin of Materials Science* **34**, 1407-1413 (2011).
55. A. Makino, H. Men, T. Kubota, K. Yubuta, A. Inoue, FeSiBPCu nanocrystalline soft magnetic alloys with high Bs of 1.9 Tesla produced by crystallizing hetero-amorphous phase. *Materials Transactions* **50**, 204-209 (2009).
56. A. D. Setyawan *et al.*, Magnetic properties of 120-mm wide ribbons of high Bs and low core-loss NANOMET® alloy. *Journal of Applied Physics* **117**, 17B715 (2015).
57. W. Mischler, G. Rosenberry, P. Frischmann, R. Tompkins, Test results on a low loss amorphous iron induction motor. *IEEE transactions on power apparatus and systems* **6**, 2907-2911 (1981).
58. Z. Wang *et al.*, Development of a permanent magnet motor utilizing amorphous wound cores. *IEEE Transactions on Magnetics* **46**, 570-573 (2010).
59. T. Fukao, A. Chiba, M. Matsui, Test results on a super-high-speed amorphous-iron reluctance motor. *IEEE Transactions on Industry Applications* **25**, 119-125 (1989).

60. R. Kolano, A. Kolano-Burian, M. Polak, J. Szynowski, Application of rapidly quenched soft magnetic materials in energy-saving electric equipment. *IEEE Transactions on Magnetics* **50**, 1-4 (2014).
61. J. M. Silveyra *et al.*, Amorphous and nanocomposite materials for energy-efficient electric motors. *Journal of Electronic Materials* **45**, 219-225 (2016).
62. S. Okamoto, N. Denis, Y. Kato, M. Ieki, K. Fujisaki, Core loss reduction of an interior permanent-magnet synchronous motor using amorphous stator core. *IEEE Transactions on Industry Applications* **52**, 2261-2268 (2016).
63. W. Tong, S. Wu, J. Sun, L. Zhu, in *Vehicle Power and Propulsion Conference (VPPC)*. (IEEE, 2016), Web **DOI:** 10.1109/VPPC.2016.7791716
64. T. Yamazakii, H. Uchiyama, K. Nakazawa, T. Isomura, H. Ogata, paper presented at the WCX™ 17: SAE World Congress Experience, 2017.
65. A. Komura *et al.*, paper presented at the Energy Efficiency in Motor Driven Systems (EEMODS) '15 Conference, Helsinski, Finland, 16 September 2015 2015.
66. N. Nishiyama, K. Tanimoto, A. Makino, Outstanding efficiency in energy conversion for electric motors constructed by nanocrystalline soft magnetic alloy "NANOMET®" cores. *AIP Advances* **6**, 055925 (2016).
67. N. Denis, M. Inoue, K. Fujisaki, H. Itabashi, T. Yano, Iron loss reduction of permanent magnet synchronous motor by use of stator core made of nanocrystalline magnetic material. *IEEE Transactions on Magnetics*, (2017).
68. "Brochure: Amorphous Metal Distribution Transformers," Hitachi Metals America, Ltd., (2016); http://metglas.com/wp-content/uploads/2016/12/Metglas-Power-Brochure.pdf.
69. "Energy Conservation Program: Energy Conservation Standards for Distribution Transformers. Final rule.," Office of Energy Efficiency and Renewable Energy, Department of Energy, (2013); https://www1.eere.energy.gov/buildings/appliance_standards/pdfs/dt_final_rule.pdf.
70. "Review and the future of amorphous metal transformers in Asia," Project4 Media Ltd., (2011); https://web.archive.org/web/20120406141302/http://www.amorphous-metal-transformer.com/ufiles/fck/file/Book%201_new_20110907.pdf.
71. E. Theisen, Development of New Amorphous and Nanocrystalline Magnetic Materials for Use in Energy-Efficient Devices. *MRS Advances*, 1-6 (2017).
72. A. H. Taghvaei, H. Shokrollahi, K. Janghorban, Properties of iron-based soft magnetic composite with iron phosphate–silane insulation coating. *Journal of Alloys and Compounds* **481**, 681-686 (2009).
73. M. Anhalt, Systematic investigation of particle size dependence of magnetic properties in soft magnetic composites. *Journal of Magnetism and Magnetic Materials* **320**, e366-e369 (2008).
74. G. Dan, X. Guoxin, L. Jianbin, Mechanical properties of nanoparticles: basics and applications. *Journal of Physics D: Applied Physics* **47**, 013001 (2014).
75. A. H. Taghvaei, H. Shokrollahi, K. Janghorban, H. Abiri, Eddy current and total power loss separation in the iron–phosphate–polyepoxy soft magnetic composites. *Materials & Design* **30**, 3989-3995 (2009).
76. J. L. Dormann, Le phénomène de superparamagnétisme. *Revue de Physique Appliquée* **16**, 275-301 (1981).
77. I. Jacobs, C. Bean, in *Magnetism*, George T. Rado, Harry Suhl, Eds. (Academic Press, New York and London, 1963), III, pp. 271-350.

78. L. Neel, Influence des Fluctuations Thermiques sur Laimantation de Grains Ferromagnetiques Tres Fins. *C R Hebd Sean Acad Sci* **228**, 664-666 (1949).
79. C. Bean, J. Livingston, Superparamagnetism. *Journal of Applied Physics* **30**, 120S-129S (1959).
80. H. Yun *et al.*, Alternate current magnetic property characterization of nonstoichiometric zinc ferrite nanocrystals for inductor fabrication via a solution based process. *Journal of Applied Physics* **119**, 113901 (2016).
81. R. J. Kaplar, J. C. Neely, D. L. Huber, L. J. Rashkin, Generation-After-Next Power Electronics: Ultrawide-bandgap devices, high-temperature packaging, and magnetic nanocomposite materials. *IEEE Power Electronics Magazine* **4**, 36-42 (2017).
82. T. Matsuda, K. Harada, H. Kasai, O. Kamimura, A. Tonomura, Observation of dynamic interaction of vortices with pinning centers by Lorentz microscopy. *Science* **271**, 1393 (1996).
83. L. Hannes, L. Michael, Electron holography—basics and applications. *Reports on Progress in Physics* **71**, 016102 (2008).
84. D. Rugar *et al.*, Magnetic force microscopy: General principles and application to longitudinal recording media. *Journal of Applied Physics* **68**, 1169-1183 (1990).
85. P. Fischer *et al.*, Imaging of magnetic domains by transmission x-ray microscopy. *Journal of Physics D: Applied Physics* **31**, 649 (1998).
86. M. Jeffrey, Progress in magnetic domain observation by advanced magneto-optical microscopy. *Journal of Physics D: Applied Physics* **48**, 333001 (2015).